Influence of structural and surface properties of Nb_2O_5 pellets on methylene blue adsorption and adsorbent reuse capacity

A. L. dos Santos[1], Á. L. S. do Amaral[1], C. R. S. Souza[1], D. C. Batista[1],
E. C. Paris[2], A. T. de Figueiredo[3], T. R. Giraldi[1]*

[1]*Universidade Federal de Alfenas, Rd. José Aurélio Vilela 11999, 37715-400, Poços de Caldas, MG, Brazil*
[2]*Laboratório Nacional de Nanotecnologia para o Agronegócio, Embrapa Instrumentação Agropecuária,*
13560-970, São Carlos, SP, Brazil
[3]*Universidade Federal de Catalão, 75704-020, Catalão, GO, Brazil*

Abstract

This study aimed to describe the preparation of Nb_2O_5 pellets by uniaxial pressing, to investigate the influence of heat treatment at different temperatures (800, 900, and 1000 °C) on the physical, surface, microstructural, and adsorptive properties of the materials, and to assess their potential as reusable adsorbents for methylene blue removal. Specimens treated at 800 °C contained a mixture of monoclinic and hexagonal phases, with a predominance of monoclinic structures. By contrast, heat treatment at 900 °C and above resulted in complete conversion to the monoclinic phase. The surface of Nb_2O_5 particles contained basic groups, possibly oxygen ions (O^-). Experimental investigations showed that methylene blue adsorption followed second-order kinetics, suggesting chemical diffusion as the dominant process. Maximum adsorption occurred at pH 6.0. Pellets remained intact after the adsorption test. A study was carried out to determine the reusability of pellets over five adsorption cycles in methylene blue solutions at different concentrations. The maximum adsorbed concentration was 10.4 mg.L^{-1}. The adsorption capacity of Nb_2O_5 specimens gradually decreased from 56% in the first cycle to 25% in the fifth cycle. Despite this reduction in removal efficiency, Nb_2O_5 pellets showed promise as reusable adsorbents in heterogeneous processes because of their high potential adsorption capacity and easy separation from the reaction medium.

Keywords: adsorption, methylene blue, niobium pentoxide, reuse.

INTRODUCTION

Niobium pentoxide (Nb_2O_5) is a highly relevant compound from a technological point of view [1]. Its remarkable chemical and physical properties make it a promising material for use in gas sensors [2], solar cells [3], electrochromic components [4], and adsorbents [5, 6]. Nb oxides have various catalytic applications [7] and can be used as an active phase [8, 9] or supports [10, 11]. Several studies have shown that Nb_2O_5 exhibits photocatalytic properties, such as selective oxidation of organic contaminants [1, 12], photodegradation of organic dyes [13, 14], and hydrogen production [15]. Nb_2O_5 contains Brønsted and Lewis acid sites and has amphoteric characteristics. When Nb_2O_5 acts as a Brønsted acid, the proton donor group is usually represented in a simplified form as an H$^+$ attached to an oxygen atom (-OH) on the oxide surface. In this case, the basic groups are oxygen ions (O^-) resulting from proton dissociation or dehydration of two terminal hydroxyls. Nb_2O_5 has been applied in catalytic reactions in which water is part of the reaction mechanism. Research has shown that the adsorption of water on Nb oxide increases Brønsted acidity and catalytic activity in isomerization reactions [16]. Lewis acid sites favor organic synthesis reactions occurring on the Nb_2O_5 surface in aqueous media [17], given that the presence of water improves oxide selectivity through changes in surface acidity [18, 19].

Although Nb_2O_5 is widely studied in catalytic reactions, there are few reports on using pure Nb_2O_5 as adsorbent material. Most studies used Nb_2O_5 combined with other oxides or in the form of composites. The effectiveness of adsorption methods is generally limited by removal efficiency. Costa et al. [20] studied the use of Nb_2O_5 combined with Al_2O_3 on a solid silica matrix prepared by a sol-gel process as an adsorbent for Cd^{2+} ions. The adsorbent exhibited high porosity and specific surface area (323 m^2.g^{-1}). The high specific surface area contributed to increasing the accessibility of adsorbent sites to Cd^{2+} ions. Furthermore, the porous silica material modified with metal oxides had high stability and showed promise for the development of new materials that adsorb metal ions. In a similar line of research, Diniz et al. [21] combined Nb_2O_5 with ZnO dispersed on a silica matrix by the sol-gel method for the adsorption of Co^{2+} ions in water and food samples. The material exhibited high surface area and had a maximum adsorption capacity of 0.518 mg.g^{-1}, showing potential as an adsorbing agent. Cavalcanti et al. [6] used zeolite-based adsorbents

impregnated with Nb_2O_5 to remove sulfur in the form of thiophene, a refractory substance difficult to remove from liquid fuels. The best adsorption results were achieved at 353 K. The reaction was best explained by a pseudo-second-order kinetic model, indicative of a chemisorption phenomenon. On the other hand, the diffusion model provided the best fit for experimental data at lower temperatures. Higher temperatures favored spontaneous processes. Nb_2O_5 in its pure form (without being combined with other materials) has been little investigated as an adsorbent. Ferreira et al. [22] used Nb_2O_5 as an adsorbent for lipases. The material was supplied by the Brazilian Metallurgy and Mining Company (CBMM) as a hydrated Nb oxide (HY-340). Heat treatment was performed at 600 °C, resulting in favorable texture characteristics and physical protection of the enzyme, as evidenced by the increased optimum temperature and improved thermal stability. The reaction was conducted at pH 6 and followed pseudo-first-order kinetics.

This study focused on the use of Nb_2O_5 for the adsorption of methylene blue dye. There is limited information in the literature regarding the use of Nb_2O_5 for methylene blue adsorption. Methylene blue is a cationic dye widely used in the textile industry and as a biological stain in histological, bacteriological, and hematological assays. If ingested, it imparts a blue color to the skin, mucous membranes, and urine [23]. If disposed of inadequately, methylene blue may contaminate aquatic environments, compromising fauna and flora. Boruah et al. [24] prepared Nb_2O_5 nanoparticles via sonication. The nanoparticles were calcined at 550 °C for 4 h to obtain pseudo-hexagonal Nb_2O_5 as a white powder. Adsorption of methylene blue followed Lagergren's pseudo-first-order kinetics. Zhang et al. [25] synthesized Nb_2O_5 nanowires by the soft chemical method using polyamide as a structure-directing agent and isopropanol as a solvent. The resulting material was used to adsorb a 20 mg.L^{-1} methylene blue solution. The adsorption capacity was about 0.17 mg.mg^{-1}. De Moraes et al. [13] obtained hydrated Nb oxide by the precipitation method and subsequently produced anhydrous niobium oxide by heat treatment of $Nb_2O_5.nH_2O$ at 550 °C for 6 h. The adsorption capacity was 20 mg.g^{-1} in 85 mg.g^{-1} methylene blue solution. The adsorption mechanism of methylene blue on Nb_2O_5 is related to the presence of Lewis and Brønsted acidic sites. Nb_2O_5 contains a combination of Nb^{5+} and O^- sites, promoting electrostatic attraction of different regions of the methylene blue molecule [26]. Nb^{5+} sites can interact with the free electron pair present in nitrogen atoms of the methylene blue molecule, and O^- sites can interact with the positive charge, which is delocalized along the molecule (resonance) [27]. Recent studies investigated different adsorbent materials for methylene blue removal, such as graphene oxide [28], silica [29], starch [30], and carbon nanotubes [15]. Table I shows some adsorbents reported in the literature specifically for methylene blue adsorption and their respective adsorption capacity (q_{max}). In most studies, adsorbents are used as suspended particles to achieve large surface areas and high mass transfer efficiencies. However, after use, it is necessary to apply complex processes for adsorbent separation,

generating additional costs and increasing treatment time. Domingos et al. [35, 36] developed ZnO materials in the form of cylinders for the decontamination of aquatic environments by photocatalysis. The materials showed high photocatalytic activity and were reused up to five times without loss of photocatalytic activity.

Table I - Previous reports of different types of adsorbents studied for methylene blue adsorption.

Adsorbent	q_{max} (mg.g^{-1})	Ref.
Graphene oxide-chitosan aerogel	110.90	[31]
TiO_2@AS	23.95	[31]
Mesoporous silica	113.64	[29]
Starch microsphere	31.95	[30]
Silica aerogels and alcogels	49.20	[32]
Carbon nanotubes	64.10	[33]
MXenes	111.11	[34]

In view of the few studies using pure Nb_2O_5 as adsorbent and the even fewer using the material in immobilized form, the current study aimed to obtain Nb_2O_5 adsorbents immobilized in the form of cylinders via pressing and applying them for methylene blue adsorption. We investigated the removal of methylene blue from aqueous solutions, assessed the influence of heat treatment temperature on the physical, structural, and adsorptive properties of Nb_2O_5 pellets, and studied the pH, kinetics, and isotherm of methylene blue adsorption. The reuse capacity of pellets was evaluated over five adsorption cycles.

MATERIAL AND METHODS

Nb_2O_5 pellets were prepared by pressing Nb_2O_5 powder. The powder material was kindly donated by CBMM. The oxide was identified as HY-340R and characterized by X-ray diffraction (XRD) after heat treatment at 800, 900, and 1000 °C (the same temperatures used for heat treatment of pellets after pressing). Analyses were performed on a diffractometer (XRD-6100, Shimadzu) at 30 kV and 30 mA using CuKα radiation and a graphite monochromator in the range of 5° to 85°. Zeta-potential analyses were performed on HY-340R powder before and after heat treatment at 900 °C. The zeta potential of suspensions was measured in the pH range of 1 to 12 using an analyzer (Zetasizer Nano, Malvern Instr.). NaOH and KCl solutions were used to adjust the pH. Sample preparation consisted of dispersing 2 mg of sample and 10 mL of water (Milli-Q) in KCl solutions, prepared from high-purity reagents, using a sonicator (Digital Sonifier, Branson). Pellets were prepared from 5.00 g of Nb_2O_5 powder, pressing it in a stainless-steel mold with an aperture diameter of 2.00 cm. First, the powder was subjected to uniaxial pressing at 131.4 kgf.cm^{-2}. Then, the resulting pellets were treated at 800, 900, or 1000 °C for 2 h at a heating rate of 10 °C.min^{-1} and cooled to room temperature.

Apparent porosity (AP, %) and apparent density (AD, g.cm^{-1}) were determined using a method based on Archimedes' principle, according to ASTM C20-00 standard (reapproved 2010), with six samples for each parameter. AP and AD were calculated from experimental data by using Eqs. A and B. The experimental procedure started with the measurement of the dry weight (W_d) of pellets after heat treatment. Then, the specimens were immersed in beakers containing water at room temperature and left to stand for 24 h. After this period, the immersed weight (W_i) was determined. Finally, the specimens were removed from the water and weighed again while wet to obtain the wet weight (W_w). All weight measurements were performed on a semi-analytical scale (AY220, Shimadzu). Linear shrinkage was calculated from the average pellet diameter (d, cm) before and after heat treatment, which was determined using the average lower (d_l) and upper (d_u) diameters of specimens, as shown in Eq. C.

$$AP = \frac{W_w - W_d}{W_w - W_i}.100 \quad \text{(A)}$$

$$AD = \frac{W_d}{W_w - W_i}.d_{water} \quad \text{(B)}$$

$$d = \frac{d_l + d_u}{2}.100 \quad \text{(C)}$$

The microstructure of pellets was examined using a scanning electron microscope (JSM 6701f, Jeol). Average grain sizes were calculated from grain diameters, measured in 100 grains per sample. Grains were selected by stratified random sampling, according to the ASTM E112 standard. Adsorption studies were conducted to evaluate the potential of Nb$_2$O$_5$ pellets as adsorbents for methylene blue removal. A 10 mg.L^{-1} solution of methylene blue (Vetec) at pH 5.8 was used for the kinetic study. Adsorption tests were performed in triplicate using 15 mL of methylene blue solution added to a beaker. Absorbance readings were taken at 663 nm from 10 to 300 min of reaction using a UV-vis spectrophotometer (Edutec). The kinetic study was conducted from 0 to 300 min. Pellets heat treated at 900 °C were kept in contact with dye solutions for 240 min (the equilibrium time, as previously determined in the kinetic study). The efficiency of samples was tested using different concentrations of methylene blue (5, 7.5, 10, 12.5, 15, and 20 mg.L^{-1}). The pH of all dye solutions was 5.8 (unadjusted pH). Finally, the pellet specimen heat-treated at 900 °C was evaluated for reusability after five adsorption cycles in methylene blue solutions at 10 mg.L^{-1}.

RESULTS AND DISCUSSION

Characterization of adsorbents

Fig. 1 illustrates the XRD patterns of unpressed Nb$_2$O$_5$ particles (HY-340R) heat-treated at 800, 900, or 1000 °C. Untreated samples and those calcined at 800 °C were composed of two Nb$_2$O$_5$ polymorphs: monoclinic (JCPDS 72-1121) and hexagonal (JCPDS 7-61) phases. The peaks of the monoclinic phase were more intense than those of the hexagonal phase. Samples calcined at 900 or 1000 °C showed peaks characteristic of the monoclinic phase only. These findings indicated that calcination at 900 °C was sufficient to fully convert the hexagonal phase to the monoclinic phase.
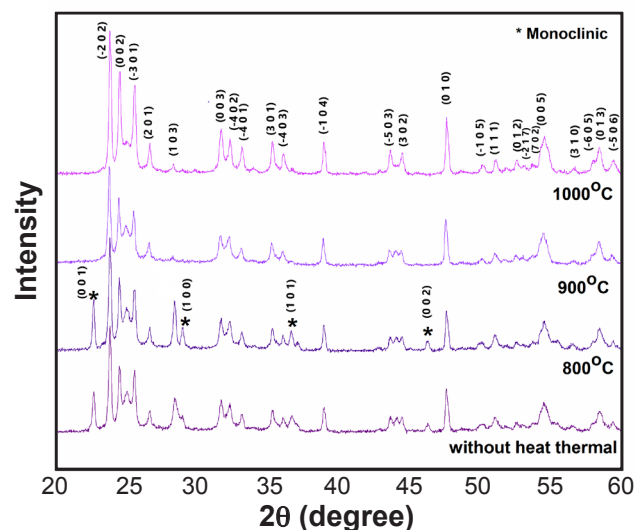

Figure 1: X-ray diffractograms of Nb$_2$O$_5$ powder particles after heat treatment at 800, 900, or 1000 °C.

Fig. 2 shows the zeta potential curves of untreated samples and samples treated at 900 °C. Note that heat treatment did not influence the surface charge of pellets, as both treated and untreated samples had an isoelectric point in the vicinity of pH 2. The surface charge became highly negative at pH values above 6.0, as shown by zeta potentials lower than -50 mV. These results indicated that the surface of Nb$_2$O$_5$ pellets contained basic groups, possibly oxygen ions (O$^-$). Such properties suggested great potential for the adsorption of cationic species, such as methylene blue. Negatively charged surfaces promote the electrostatic attraction of
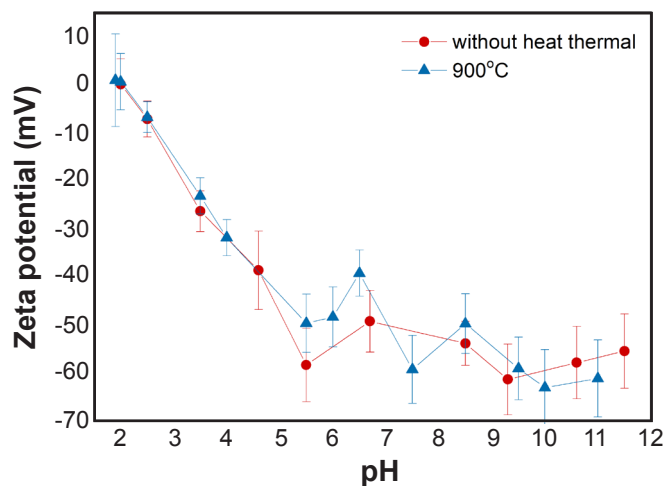

Figure 2: Zeta potential as a function of pH of Nb$_2$O$_5$ pellets before and after heat treatment at 900 °C.

Table II - Physical properties of Nb_2O_5 pellets treated at 800, 900, or 1000 °C.

Heat treatment temperature (°C)	Apparent porosity (%)	Apparent density (g.cm⁻³)	Linear shrinkage (%)	Surface area (m².g⁻¹)
800	47.13±0.89	2.85±0.01	6.57±0.37	0.28
900	45.97±0.08	2.82±0.02	9.58±0.38	0.24
1000	46.59±0.78	2.87±0.01	17.72±0.26	0.22

positively charged species, favoring the adsorption process.

Table II presents the apparent porosity, apparent density, linear shrinkage, and surface area of pellets treated at different temperatures. There was an increase in linear shrinkage as heat treatment temperature increased. However, heat treatment had no significant effects on apparent porosity or apparent density. These findings can be explained by the fact that pellet specimens did not undergo densification, given that the sintering temperature of Nb_2O_5 is above 1250 °C [37]. It can also be seen from Table II that the average porosity of samples was about 46%. This value indicated a highly porous material (apparent porosity >45%), which is desirable for adsorbents. The surface area was low for all samples, explained by the fact that samples were pelleted.

Fig. 3 shows the electron micrographs of Nb_2O_5 pellets after heat treatment at 800, 900, or 1000 °C. A heterogeneous morphology was observed, with variations in grain and pore sizes. The mean grain size increased with increasing heat treatment temperature, as the particle coalescence occurred. Thus, the average particle size increased markedly, particularly in samples treated at 1000 °C, with values of 453, 454.1, and 513.5 nm for pellets heat-treated at 800, 900, and 1000 °C, respectively. Such an increase in grain size explained the increase in linear shrinkage (Table II). However, it was not sufficient to promote pellet

densification. Particle size histograms confirmed the trend toward increased particle size with increasing temperatures.

Adsorption assays

Fig. 4 shows the adsorption capacity of samples as a function of pH. It was observed that methylene blue adsorption was highest at pH 6.0. This result may be associated with the zeta potential of samples (lower than -50 mV, Fig. 2), which indicated that the surface charge of Nb_2O_5 became highly negative at pH values above 6.0. As such, the surface of Nb_2O_5 pellets contained basic groups, possibly oxygen ions (O⁻), which favored the adsorption of cationic species, such as methylene blue. On the other hand, pH values greater than 6.0 led to a decrease in adsorption. This decreasing trend in adsorption might be due to the overcrowding of HO⁻ ions in the solution. Thus, at the optimum pH of 6.0, the solution environment was highly favorable for the interaction of methylene blue cations with the Nb_2O_5 surface. In analyzing the effect of heat treatment temperature on methylene blue adsorption, it was observed that the sample treated at 900 °C achieved higher adsorption percentages, that is about 95% at pH 6.0. Although apparent porosity was similar between samples, it is believed that the sample treated at 800 °C had a smaller adsorption capacity
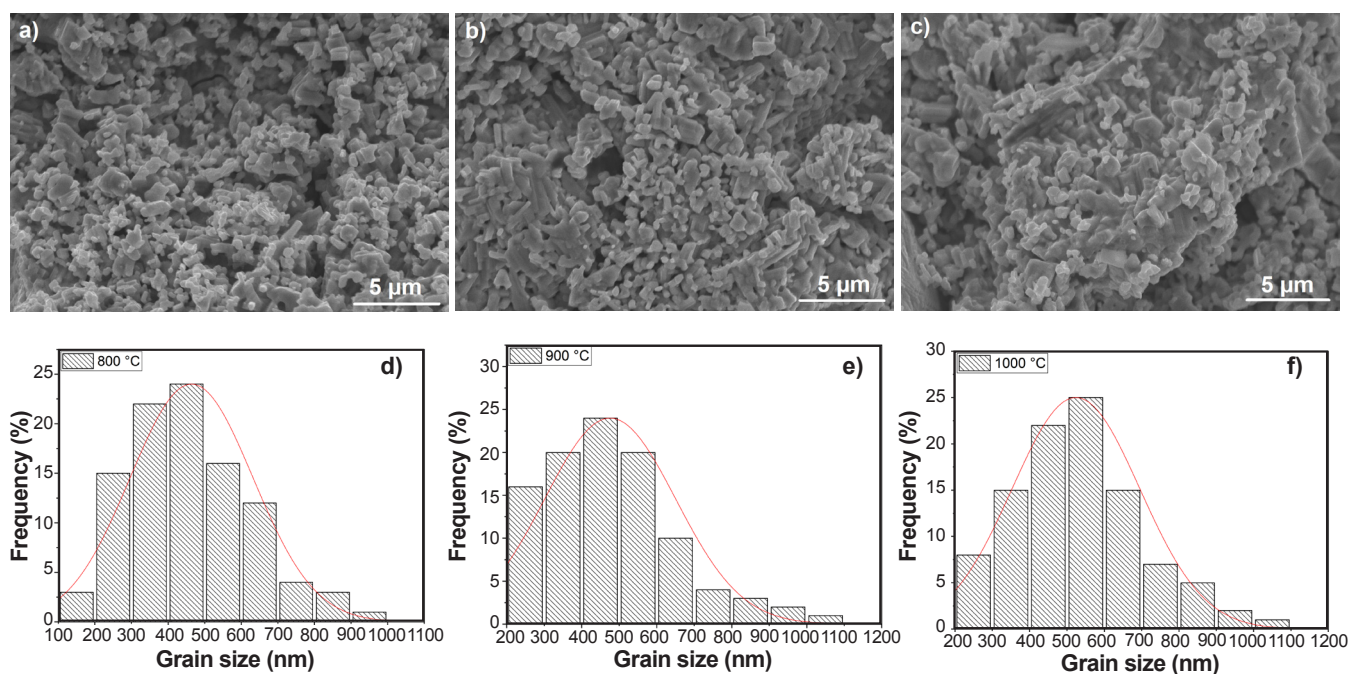

Figure 3: Scanning electron micrographs of Nb_2O_5 pellets obtained at 800 °C (a), 900 °C (b), or 1000 °C (c) and their respective particle size distribution curves (d,e,f).
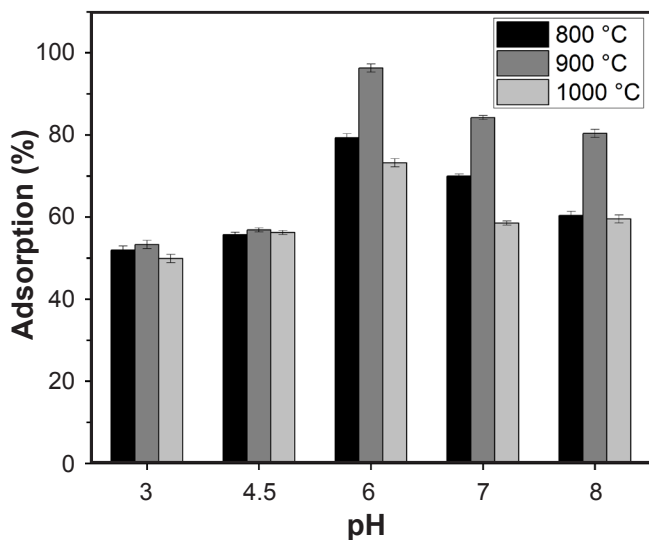
Figure 4: Methylene blue (MB) adsorption percentage as a function of pH, with an initial MB concentration of 10 mg.L^{-1} and a reaction time of 240 min.

than that treated at 900 °C because of its hexagonal phase, which was not identified in the other samples. This fact might have hindered the adsorption capacity of the sample treated at 800 °C. The lower adsorption capacity of the sample treated at 1000 °C, on the other hand, might be related to its higher density.

The adsorption capacity of Nb$_2$O$_5$ pellets was evaluated by varying adsorbate concentration and the contact time between adsorbent and adsorbate. Methylene blue was used at a concentration of 10 mg.L^{-1}. Fig. 5 shows the adsorption percentage of methylene blue as a function of contact time and the results of the kinetic study. The adsorption/desorption equilibrium was reached after about 240 min of contact for the Nb$_2$O$_5$ pellet treated at 900 °C, which was the sample with the highest adsorption capacity. After this period, methylene blue concentration remained constant. However, not all samples reached equilibrium at 240 min. Samples treated at 800 or 1000 °C did not reach equilibrium at the time limit (300 min). These findings further indicated that the sample obtained at 900 °C had the best adsorption properties. In fact, at 240 min of reaction, pellets heat-treated at 800, 900, or 1000 °C achieved adsorption percentages of 80.6%, 97.7%, and 84.0%, respectively. For all samples, variations in adsorption decreased with time until equilibrium was achieved. This factor might be associated with the availability of active sites throughout adsorption; over time, the sites were occupied by methylene blue molecules, leading to a constant occupancy rate from 240 min of reaction onward. Such a trend was made evident by the adsorption curve.

Several models can be used to explain reaction kinetics and identify adsorption mechanisms, which involve diffusion control and mass transfer [38]. The most frequent models are pseudo-first-order [39] and pseudo-second-order [40]. Experimental data were well-fitted by a pseudo-second-order model (Fig. 5b). The pseudo-first-order model did not provide a good fit for the experimental data. The pseudo-
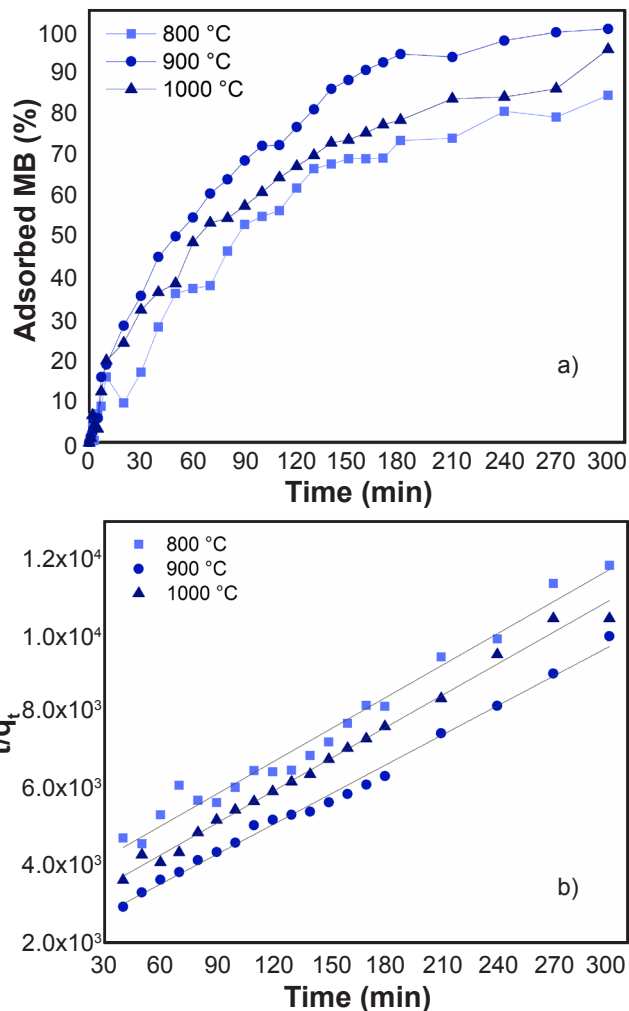

Figure 5: Graphs of: a) methylene blue (MB) adsorption percentage as a function of time at pH 5.8 (initial MB concentration of 10 mg.L^{-1}); and b) adsorption kinetics.

second-order kinetic model was developed by Ho et al. [40] and is described by:

$$\frac{dq_t}{d_t} = k_2(q_E - q_t)^2 \tag{D}$$

where k_2 (g.mg^{-1}.min^{-1}) is the rate constant of the pseudo-second-order adsorption reaction and q_e (mg.g^{-1}), and q_t (mg.g^{-1}) are the concentrations of adsorbate retained on the adsorbent at equilibrium and time t, respectively. By integrating Eq. D and applying boundary conditions (q_t=0, t=0; when q=q_t, t=t), we obtain:

$$\frac{1}{q_E - q_t} = \frac{1}{q_E} + k_2.t \tag{E}$$

and linearization of Eq. E results in the following equation:

$$\frac{t}{q_t} = \frac{t}{k_2.q_e^2} + \frac{t}{q_e} \tag{F}$$

The values of q_e and k_2 can be obtained from the intercept

and slope of the $\frac{t}{q_t} \cdot t$ curve (Fig. 5b). If the pseudo-second-order model is applicable, $\frac{t}{q_t} \cdot t$ the plot should have a linear relationship (~1), as was observed for all Nb_2O_5 pellets. The R^2 was 0.977, 0.993, and 0.992 for pellets treated at 800, 900, and 1000 °C, respectively. The model is related to the adsorption capacity of the adsorbent, and it considers that the number of active sites on the adsorbent surface is directly proportional to the adsorption rate. Thus, factors such as the amount of adsorbate on the adsorbent surface and the amount of adsorbate in equilibrium can alter the reaction speed [41]. From model fitting and linear regression results, it was possible to obtain the theoretical values for adsorption capacity at equilibrium (q_e) and adsorption rate constant (k_2, Eq. D), as shown in Table III. The pseudo-second-order kinetic model best fitted experimental data, as the R^2 was close to 1.

Table III - Theoretical values of adsorption kinetic parameters.

Heat treatment temperature (°C)	K (min^{-1})	q_e	R^2
800	0.229	0.0241680	0.978
900	0.334	0.0293101	0.993
1000	0.289	0.0251964	0.992

K: adsorption rate constant; q_e: adsorption capacity at equilibrium; R^2: coefficient of determination.

The influence of methylene blue concentration on adsorption was investigated by varying the concentration from 5 to 20 mg.L^{-1}. Fig. 6a illustrates the decolorization percentage of solutions, and Fig. 6b shows the concentration of adsorbed dye. In reactions with an initial dye concentration of 10 mg.L^{-1}, the highest decolorization percentage was 61% for pellets treated at 800 °C, 66% for pellets treated at 900 °C, and 67% for pellets treated at 1000 °C (Fig. 5a). However, it was observed that the concentration of adsorbed methylene blue (Fig. 6b) increased with increasing initial dye concentration. The maximum concentration of adsorbed methylene blue was 10.4 mg.L^{-1} for all samples. This high adsorption capacity is explained by the fact that methylene blue is a cationic molecule and Nb_2O_5 has basic groups composed of oxygen ions (O$^-$) on its surface. Thus, there is a high affinity between adsorbent and adsorbate, resulting in high adsorption capacity. Fig. 7 shows a representative photograph of Nb_2O_5 pellets before and after adsorption. It can be said that the material is suitable for the adsorption of cationic dyes, such as methylene blue.

Five adsorption cycles lasting 4 h each were performed with pellets treated at 900 °C for evaluation of adsorbent reusability, as depicted in Fig. 8a. The samples gradually lost their adsorption capacity, starting from 56% in the first cycle and decreasing to 25% in the fifth cycle. Despite the decrease in adsorption capacity, the material showed significant reusability, as it provided relevant dye removal after five cycles. It should be noted that there is a strong trend toward the conversion of homogeneous to heterogeneous processes because of the reduced effort in separating solid materials from the reaction medium [35]. During the reuse cycles, the test specimens were chemically and thermally stable and had sufficient mechanical strength for dye removal. The XRD pattern of the sample after reuse (Fig. 8b) showed that the monoclinic structure remained.
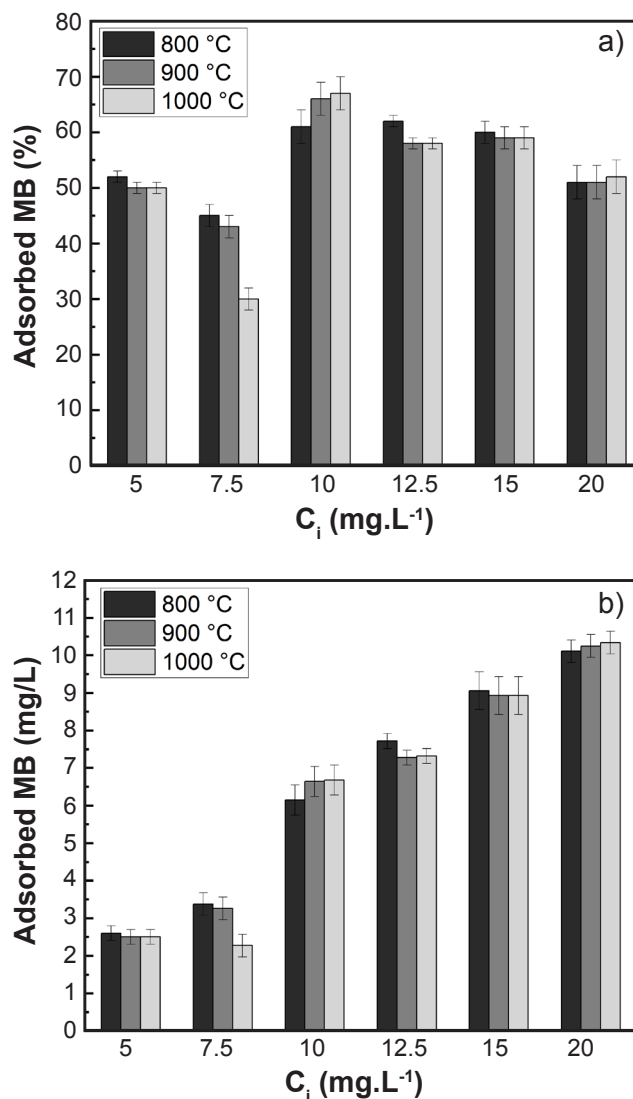

Figure 6: Results of adsorption of solutions containing different concentrations of methylene blue by Nb_2O_5 pellets treated at 900 °C, pH 5.8, and 240 min of contact: a) decolorization percentage; and b) concentration of adsorbed dye.

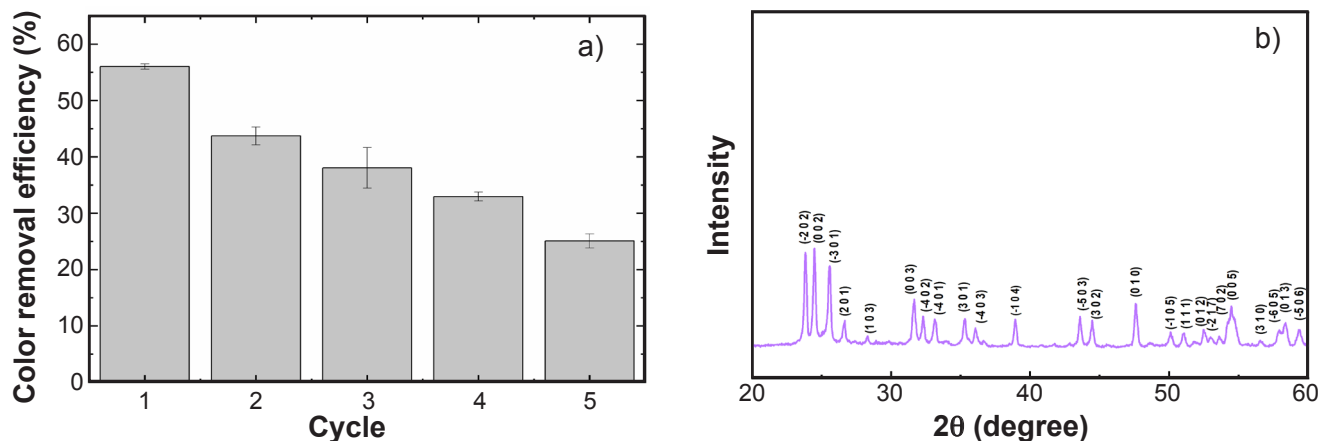Figure 7: Representative photograph of Nb_2O_5 pellets before and after adsorption of methylene blue.

Figure 8: Percentage of MB removal as a function of the number of consecutive adsorption cycles (a), and X-ray diffractogram of Nb_2O_5 after reuse (b).

CONCLUSIONS

Nb_2O_5 pellets obtained by pressing were shown to have great potential for the removal of dyes via adsorption. Samples were composed of Nb_2O_5 with a monoclinic and hexagonal phase mixture, which was fully converted to monoclinic by heat treatment at 900 °C and above. Pellets had negatively charged adsorptive sites and 500 nm sized grains. Samples exhibited high decolorization efficiency for methylene blue solutions. The optimum pH for adsorption was 6.0. The adsorption mechanism followed second-order kinetics, and the increase in dye concentration did not affect the adsorption performance of pellets. Pellets were easily removed from the medium and showed good reusability for up to five adsorption cycles. During reuse cycles, pellets were chemically and thermally stable, having sufficient mechanical strength for dye removal. Adsorbents in pellet form are environmentally advantageous because of their high reuse and recycling potential. By contrast, particulate materials may become an environmental liability with high treatment costs.

REFERENCES

[1] E.T. de Jesus, A.J. Moreira, M.C. Sá, G.P.G. Freschi, M.R. Joya, M.S. Li, E.C. Paris, Environ. Sci. Pollut. Res. **28** (2021) 69401.
[2] H.G. Moon, H.W. Jang, J.S. Kim, H.H. Park, S.J. Yoon, Sens. Actuators B Chem. **153**, 1 (2011) 37.
[3] D.D. Yao, R.A. Rani, A.P. O'Mullane, K. Kalantar-Zadeh, J.Z. Ou, J. Phys. Chem. C **118**, 1 (2014) 476.
[4] C. Yu, D. Ma, Z. Wang, L. Zhu, H. Guo, X. Zhu, J. Wang, Ceram. Int. **47**, 7 (2021) 9651.
[5] L.A. Rodrigues, M.L.C.P. da Silva, Quim. Nova **32**, 5 (2009) 1206.
[6] R.M. Cavalcanti, I.C.L. Barros, J.A. Dias, S.C.L. Dias, J. Braz. Chem. Soc. **24**, 1 (2013) 40.
[7] K. Tanabe, Catal. Today **78** (2003) 65.
[8] M.O. Guerrero-Pérez, Catal. Today **354** (2020) 19.
[9] E. Rojas, J.J. Delgado, M.O. Guerrero-Pérez, M.A. Bañares, Catal. Sci. Technol. **3**, 12 (2013) 3173.
[10] A.M. Jasim, G. Xu, S. Al-Salihi, Y. Xing, ChemistrySelect **5**, 37 (2020) 11431.
[11] Y. Li, S. Yan, W. Yang, Z. Xie, Q. Chen, B. Yue, H. He, J. Mol. Catal. A Chem. **226**, 2 (2005) 285.
[12] O.F. Lopes, E.C. Paris, C. Ribeiro, Appl. Catal. B **144** (2014) 800.
[13] N.P. de Moraes, F.N. Silva, M.L.C.P. da Silva, T.M.B. Campos, G.P. Thim, L.A. Rodrigues, Mater. Chem. Phys. **214** (2018) 95.
[14] N.T. do Prado, L.C.A. Oliveira, Appl. Catal. B **205** (2017) 481.
[15] X. Chen, T. Yu, X. Fan, H. Zhang, Z. Li, J. Ye, Z. Zou, Appl. Surf. Sci. **253**, 20 (2007) 8500.
[16] Q.L. Dai, B. Yan, Y. Liang, B.Q. Xu, Catal. Today **295** (2017) 110.
[17] K. Nakajima, Y. Baba, R. Noma, M. Kitano, J.N. Kondo, S. Hayashi, M. Hara, J. Am. Chem. Soc. **133** (2011) 4224.
[18] K. Omata, K. Matsumoto, T. Murayama, W. Ueda, Catal. Today **259** (2015) 205.
[19] K. Omata, K. Matsumoto, T. Murayama, W. Ueda, Chem. Lett. **43**, 4 (2014) 435.
[20] L.M. Costa, E.S. Ribeiro, M.G. Segatelli, D.R. do Nascimento, F.M. de Oliveira, C.R.T. Tarley, Spectrochim. Acta B **66**, 5 (2011) 329.
[21] K.M. Diniz, F.A. Gorla, E.S. Ribeiro, M.B.O. do Nascimento, R.J. Corrêa, C.R.T. Tarley, M.G. Segatelli, Chem. Eng. J. **239** (2014) 233.
[22] R.D.M. Ferreira, R. Brackmann, E.B. Pereira, R.D.C.

da Rocha, Biocatal. Agric. Biotechnol. **30** (2020) 101812.

[23] B. Coulibaly, A. Zoungrana, F.P. Mockenhaupt, R.H. Schirmer, C. Klose, U. Mansmann, P.E. Meissner, O. Müller, PLoS One **4**, 5 (2009) e5318.

[24] B. Boruah, R. Gupta, J.M. Modak, G. Madras, Nanoscale Adv. **1**, 7 (2019) 2748.

[25] Z. Zhang, J. Zhang, Y. Chuanjun, H. Jianheng, Z. Shifu, Micro Nano Lett. **13**, 2 (2018) 175.

[26] F.D. Troncoso, G.M. Tonetto, Sustain. Environ. Res. **31**, 1 (2021) 35.

[27] W. Avansi, V.R. de Mendonça, O.F. Lopes, C. Ribeiro, RSC Adv. **5**, 16 (2015) 12000.

[28] Y. Shi, G. Song, A. Li, J. Wang, H. Wang, Y. Sun, G. Ding, Colloids Surf. A Physicochem. Eng. Asp. **641** (2022) 128595.

[29] C.Q. Huang, X. Zhang, D.C. Qiu, H.J. Wei, Adv. Mater. Res. **557-559** (2012) 427.

[30] X.P. Huo, F. Wang, D. Deng, L. Wang, Adv. Mater. Res. **557-559** (2012) 1109.

[31] Y. Geng, J. Zhang, J. Zhou, J. Lei, RSC Adv. **8**, 57 (2018) 32799.

[32] N. Saad, M. Al-Mawla, E. Moubarak, M. Al-Ghoul, H. El-Rassy, RSC Adv. **5**, 8 (2015) 6111.

[33] D. Zhao, Y. Ding, S. Chen, T. Bai, Y. Ma, Asian J. Chem. **25**, 10 (2013) 5756.

[34] Y. Lei, Y. Cui, Q. Huang, J. Dou, D. Gan, F. Deng, M. Liu, X. Li, X. Zhang, Y. Wei, Ceram. Int. **45**, 14 (2019) 17653.

[35] G.H.S. Domingos, T.M.O. Ruellas, L.O.O. Peçanha, J.O.D. Malafatti, E.C. Paris, S.C. Maestrelli, T.R. Giraldi, Int. J. Appl. Ceram. Technol. **18**, 3 (2021) 622.

[36] T.M.O. Ruellas, L.O.O. Peçanha, G.H.S. Domingos, C.R. Sciena, J.O.D. Malafatti, E.C. Paris, S.C. Maestrelli, T.R. Giraldi, Environ. Technol. **42**, 12 (2021) 1861.

[37] J. Dong, M. Kermani, C. Hu, S. Grasso, J. Asian Ceram. Soc. **9**, 3 (2021) 934.

[38] K.L. Tan, B.H. Hameed, J. Taiwan Inst. Chem. Eng. **74** (2017) 25.

[39] Y.S. Ho, G. McKay, Process Saf. Environ. Prot. **76**, 2 (1998) 183.

[40] Y.S. Ho, J.C.Y. Ng, G. McKay, Sep. Purif. Methods **29**, 2 (2000) 189.

[41] F.H.M. Souza, V.F.C. Leme, G.O.B. Costa, K.C. Castro, T.R. Giraldi, G.S.S. Andrade, Water Air Soil Pollut. **231** (2020) 242.